

## NUMERICAL FLUID DYNAMICAL ANALYSIS OF SOLID OXIDE FUEL CELLS (SOFC)

**Samuel Tadeu de Paula Andrade, samuelt@ufmg.br**

Dep. de Engenharia Mecânica – DEMEC – UFMG – Av. Antônio Carlos, 6627, 31270-901, Pampulha, Belo Horizonte, MG, Brasil

**Rosana Zacarias Domingues, rosanazd@ufmg.br**

Laboratório de Materiais e Pilhas a Combustível – LaMPaC – DQ – UFMG – CEMIG

**Ramon Molina Valle, ramon@demec.ufmg.br**

Mobility Technological Center. Dep. de Engenharia Mecânica – DEMEC – UFMG – Av. Antônio Carlos, 6627, 31270-901, Pampulha, Belo Horizonte, MG, Brasil

**Marcos Vinicius Bortolus, borta@demec.ufmg.br**

Dep. de Engenharia Mecânica – DEMEC – UFMG – Av. Antônio Carlos, 6627, 31270-901, Pampulha, Belo Horizonte, MG, Brasil

**Abstract.** *The computational modeling plays an important role on the project, the design and the evaluation of the Solid Oxide Fuel Cell (SOFC) performance. However, due to the large quantity of double physical phenomena, this modeling shows great complexity. Besides this interdependence, the validation of these models represents a problem because of the small dimensions of these devices, which make it difficult the obtaining of experimental data. In this work, a stack designed on laboratory has its flow and pressure profiles evaluated tri-dimensionally. Through this method, the momentum equations are solved by finite volume technique using a commercial software. It is considered steady state and isotropy to all physical properties, which are determined on constant temperature. The model validation is performed through its two dimensional versions, based on published literature results. The stack, in this case, has ten cells associated in a serial way. The results indicate some heterogeneity on flow between cells and flow distribution nearly homogeneous along each cell. The pressures increase in a asymptotic way at manifolds.*

**Keywords:** *SOFC, interconnects, stacks, modeling, finite volume method*

### 1. INTRODUCTION

The fuel cells that are power generators are highly efficient. They are decentralized and could use fuel from different sources, including the renewable ones.

The cells are formed by unitary cells structured by an electrolyte, an anode and a cathode linked by interconnects forming a stack. The interconnects for planar SOFC (Solid Oxide Fuel Cell) are plates that make possible each cell to be linked to other in a serial association. Thus, the currents are summed, and consequently, the available power is adjusted to the desired power. The electrical charges do not interfere on gas stream inside of SOFC, because the charges moves only on system solid parts, such as electrodes and interconnects.

Vandersteen *et al.* (2004) carried out a short revision of equations involved on SOFC general modeling. He presented ten unsolved problems until the publication date, related to SOFC modeling. Kakaç *et al.*, (2007) carried out an extended and detailed revision of macro and micro SOFC modeling.

One-dimensional, two-dimensional and tridimensional equations could be based on the developed work by Bove and Ubertini (2005).

The use of FLUENT software as SOFC modeling tool was published by Autissier *et al.* (2003); Zitney *et al.* (2004); Van Herle *et al.* (2005); Gubner *et al.* (2006); Yokoo *et al.* (2008) and Andrade *et al.* (2008). Others kinds of software are also used such as the STAR-CD and ANSYS by Yakabe *et al.* (1999), Chyou *et al.* (2005).

Van Herle *et al.* (2005) shows how the flow distribution in a stack could impact on the electrical power. He proposed modifications on the stack design through a flow analysis using the finite volume technique. These modifications resulted on a smaller heterogeneity on flow distribution, leading to a better stack performance. Gubner *et al.* (2006) focuses on the efforts to obtain a smaller level of heterogeneity along each of stack interconnect. He carried out an analysis by the finite volume technique and proposed modifications on the interconnect design.

In this work, the main objectives are the search to evaluate the flow distribution between the interconnects of a stack and along each of the interconnects. This stack is under developing at LaMPaC. For this reason, it was developed by a tridimensional model applying the volume finite technique with auxiliary of the FLUENT software. The model was validated by an experimental data available on literature Costamagna *et al.*, (1994). However, on the validation process, a simplification for a two-dimensional model was done.

## 2. METHODOLOGY

### 2.1. Mathematical Model

The flow modeling on stack is based on the solution of momentum conservation equations. These are non-linear partial differential equations. These equations describe the velocity and the pressure of a fluid on time and space. As in the work, the fluid considered is Newtonian (in this case, the air), these equations are simplified, becoming the Navier-Stokes equations. They are written for each canonical direction.

- For “x” direction

$$\rho \frac{Du}{Dt} = \rho g_x - \frac{\partial p}{\partial x} + \frac{\partial}{\partial x} \left[ \mu \left( 2 \frac{\partial u}{\partial x} - \frac{2}{3} \nabla \cdot \vec{V} \right) \right] + \frac{\partial}{\partial y} \left[ \mu \left( \frac{\partial u}{\partial y} + \frac{\partial v}{\partial x} \right) \right] + \frac{\partial}{\partial z} \left[ \mu \left( \frac{\partial w}{\partial x} + \frac{\partial u}{\partial z} \right) \right] \quad (1)$$

- For “y” direction

$$\rho \frac{Dv}{Dt} = \rho g_y - \frac{\partial p}{\partial y} + \frac{\partial}{\partial y} \left[ \mu \left( 2 \frac{\partial v}{\partial y} - \frac{2}{3} \nabla \cdot \vec{V} \right) \right] + \frac{\partial}{\partial x} \left[ \mu \left( \frac{\partial u}{\partial y} + \frac{\partial v}{\partial x} \right) \right] + \frac{\partial}{\partial z} \left[ \mu \left( \frac{\partial v}{\partial z} + \frac{\partial w}{\partial y} \right) \right] \quad (2)$$

- For “z” direction

$$\rho \frac{Dw}{Dt} = \rho g_z - \frac{\partial p}{\partial z} + \frac{\partial}{\partial z} \left[ \mu \left( 2 \frac{\partial w}{\partial z} - \frac{2}{3} \nabla \cdot \vec{V} \right) \right] + \frac{\partial}{\partial y} \left[ \mu \left( \frac{\partial v}{\partial z} + \frac{\partial w}{\partial y} \right) \right] + \frac{\partial}{\partial x} \left[ \mu \left( \frac{\partial w}{\partial x} + \frac{\partial u}{\partial z} \right) \right] \quad (3)$$

Where:

u, v e w are velocities [m/s] on directions x, y e z, respectively;

V is the velocity vector [m/s];

μ is the fluid dynamic viscosity [Pa s];

ρ is the fluid density [kg/m<sup>3</sup>];

g is the gravity acceleration in given direction [m/s<sup>2</sup>];

t is a given time instant [s].

The following simplifications are also applied on Eq. (1), (2) and (3):

- Steady state;
- Laminar stream;
- Incompressible stream.

#### 2.1.1. Physical Domain

The stack is characterized by the use of metallic interconnects. The basic dimensions of each one of them are 80 mm x 40 mm x 1 mm. The Fig. 1 shows an isometric view of the physical domain that is related to the studied stack.

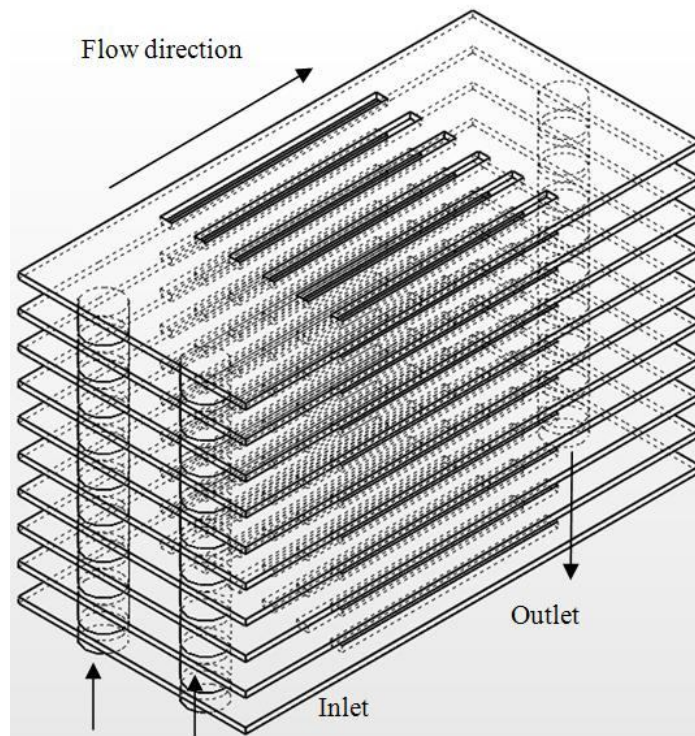


Figure 1: Isometric view of the physical domain.

### 2.1.2. Computational Domain

Based on the great aspect ratio of physical domains, it is necessary to simplify it to reduce the consume of computational resources. Therefore, the physical domain is sliced by its longitudinal plane, resulting on computational domains as shown in the Fig. 2. This is possible because this domain has a geometrical symmetry and the stream has a physical symmetry.

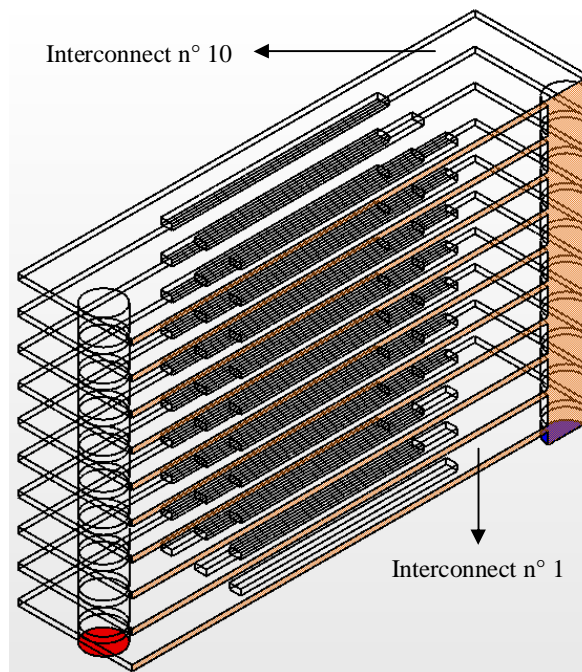


Figure 2: Isometric view. It is highlighting the main boundary conditions.

### 2.1.3. Boundary Conditions

In the Fig. 2, the mass inlet boundaries in which a value of  $1,0208 \times 10^{-4}$  kg/s is applied is marked in red. This mass flow is equal to 0,5 L/min for each cell. In the Fig. 2 the outlet boundary is marked in dark blue. There the boundary condition of prescribed pressure equal to 0 kPa is applied. The place marked in amber corresponds to the physical domain which was sliced. In this area, the symmetry boundary condition is applied. In all others boundaries the non-slip condition is applied.

### 2.2. Numerical Model

For the solution of momentum conservation equations, the volume finite technique is utilized. This technique was developed originally by Suhas Patankar. Its formulation is based on partially differential equations for a given physical phenomenon, and their physical interpretations on the control volume concept. This technique seeks to discrete the domains and the differential equations, transforming them into algebraic equations. The detailed description of this method is in Malalasekera (1995) and Patankar (1980) approaches.

The FLUENT is a commercial software that has been improved throughout the years. In this work, its 6.3.26 version was used and this version utilizes the finite volume technique as a basis for the solution of partial differential equations. It is also very flexible and general-purpose computational fluid dynamics software. FLUENT is able to solve equations by two ways: coupled and segregated. It has some interpolation models, as upwind and power-law; and some pressure-velocity couplings, such as SIMPLE, SIMPLEC and QUICK.

The SIMPLE algorithm was used to the pressure-velocity coupling and to the Power-Law interpolation algorithm. (Malalasekera (1995) and Patankar (1980) considering the under relaxation coefficient equal to 0.1 and 30,000 iterations.

The mesh density influence was evaluated by volume edge dimensions, varying from 1 mm to 0.2 mm. A non-structured mesh was used because of the computational domain complexity.

### 2.3. Applied Validation

The model validation was done by the basis of results obtained by Costamagna *et al.* (1994). The authors constructed a stack of interconnects represented in the Fig. 3. This stack has 100 interconnects and the work fluid is the air, supplied by a blower with a mass flow of 0,097 kg/s.

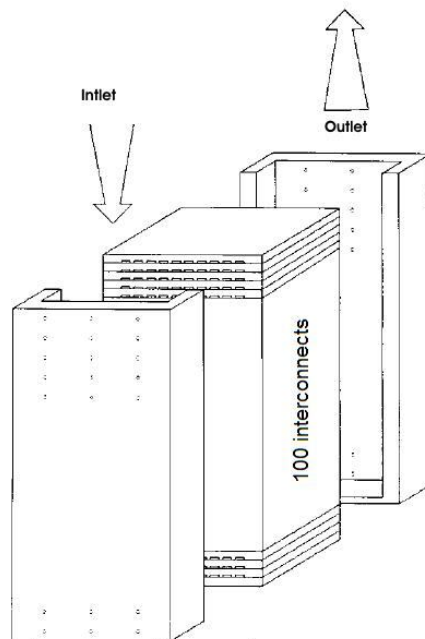


Figure 3: Device Schematic view, adapted from Costamagna *et al.* (1994).

The 14 first interconnects had their intlets blocked by a mesh, placed at the admission of inlet manifold. It was carried out in order for inlet disturbance effects to be eliminated from measures. The experiment consists on

measurements of the pressure on inlet and outlet from each of the interconnects along the inlet and outlet manifolds. The authors noted that the pressure did not vary along each of interconnects width. The mass flow on each interconnect outlet was also measured.

Due to these results, the validation of the proposed model is done through a two-dimensional version of device created by Costamagna *et al.* (1994). This two-dimensional domain version is shown in the Fig. 5 with more significant dimensions indicated.

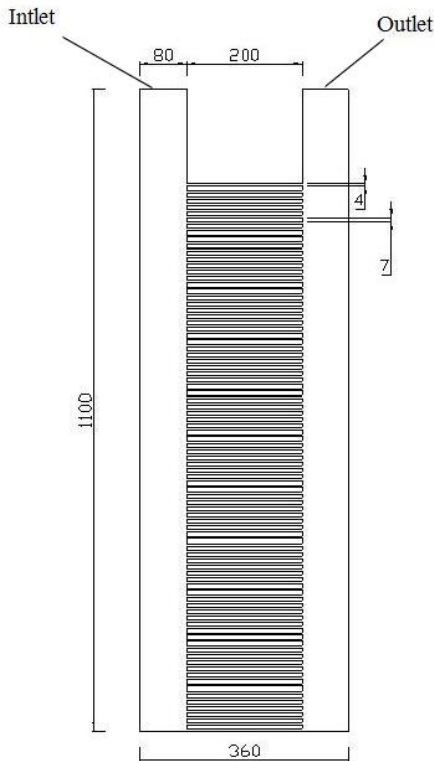


Figure 4: Two-dimensional version of the device of Costamagna *et al.* (1994), dimensions in millimeters.

A constant velocity equal to 4,04 m/s is applied on the device inlet. It is equivalent to the mean velocity related to the tridimensional domain. On the outlet device the boundary condition of prescribed gauge pressure equal to 0 kPa is applied. All numerical parameters used on the validation are those described in section 2.2.

#### 2.4 Mesh tests

A preliminary study is carried out to eliminate the mesh influence on the results of the flow distribution. Meshes with edges equal to 1 mm, 0.5 mm, 0.25 mm and 0.20 mm are used in this study. These meshes are unstructured and mainly composed of tetrahedra.

The results are presented as a function of the interconnect number. By the Fig.2, the interconnect 1 corresponds to that nearer to the inlet and outlet stack. The interconnect 10 is placed on top of stack. The Fig. 5 shows the flow distribution for each one utilized mesh along 10 interconnects.

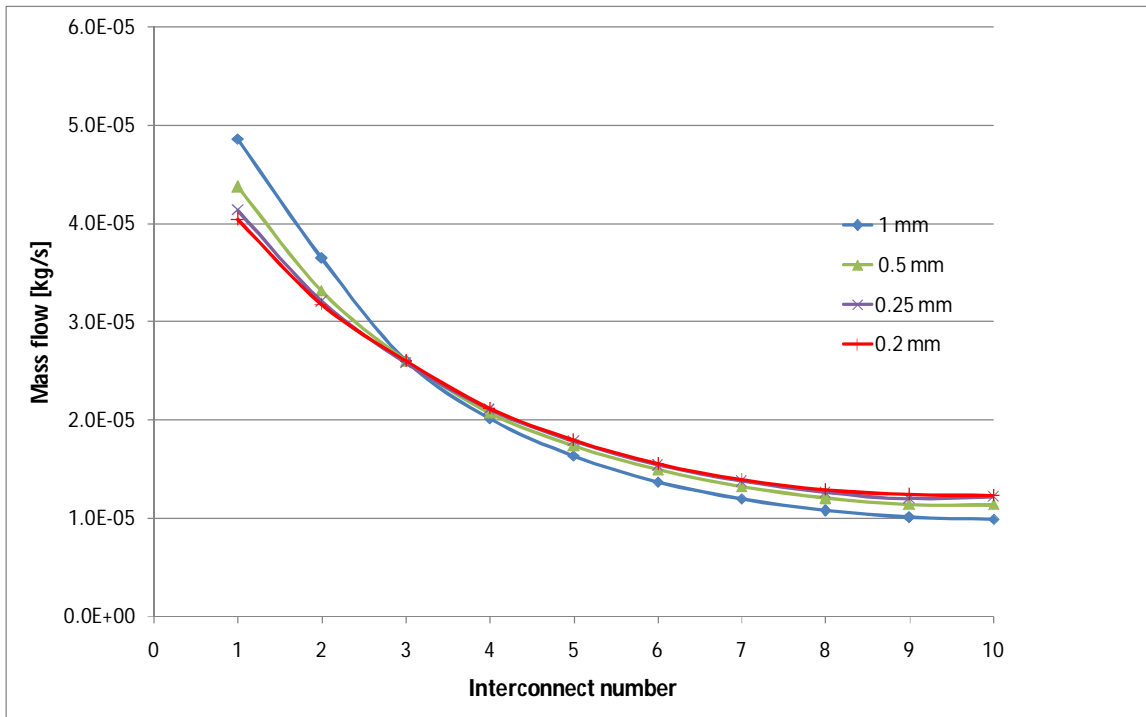


Figure 5: Comparison between model results for several meshes.

It is possible to notice, through different meshes, that the curves behavior is similar. Nevertheless, the coarsest mesh has bigger flows on the first interconnects.

The Fig. 6 shows the relative error for the flow related to the finest mesh result, from 1 mm to 0.25 mm meshes, concerning the interconnect number.

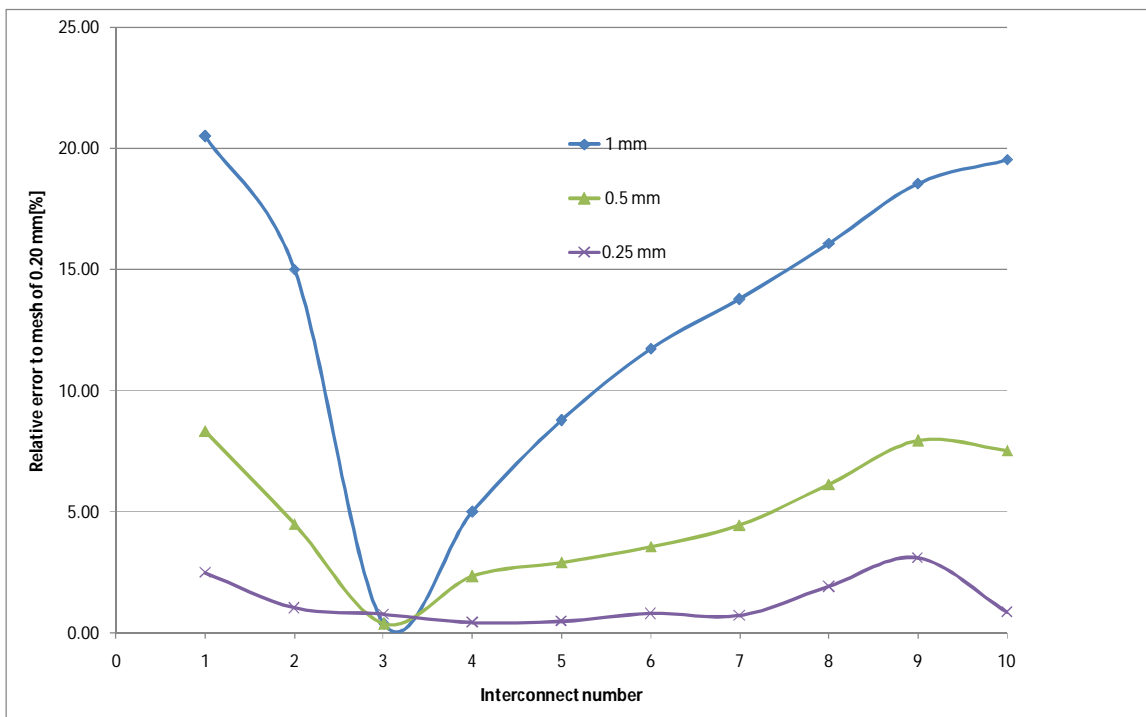


Figure 6: Comparison between relative errors for several meshes.

It was expected that the finer mesh would be that one with the best result. It is possible to notice that the coarsest mesh has errors up to 20% superior to the finer mesh. The 0.25 mm mesh (the second finest) presents inferior errors to 5%. It is interesting to note that all of them tend to present smaller errors on interconnect number 3.

It is possible to achieve better results than these refining more the mesh. However, the computational resources available on the laboratory are not enough for this procedure.

As the 0,25 mm mesh presents low errors if compared to finest mesh. It is elated as the mesh that could be used in the model without interfere on results. Moreover, the consume of computational resources for the finest mesh is very large.

### 3. RESULTS

#### 3.1. Validation

The flow on each of the interconnect outlets is obtained from the velocity field. These flows are calculated by the integration of velocity profiles obtained on outlet interconnects. The Fig.7 shows the results of this process, where the flow is for the interconnect number. The interconnect number 100 is on the device base, whereas the number 15 is near to device inlet and outlet.

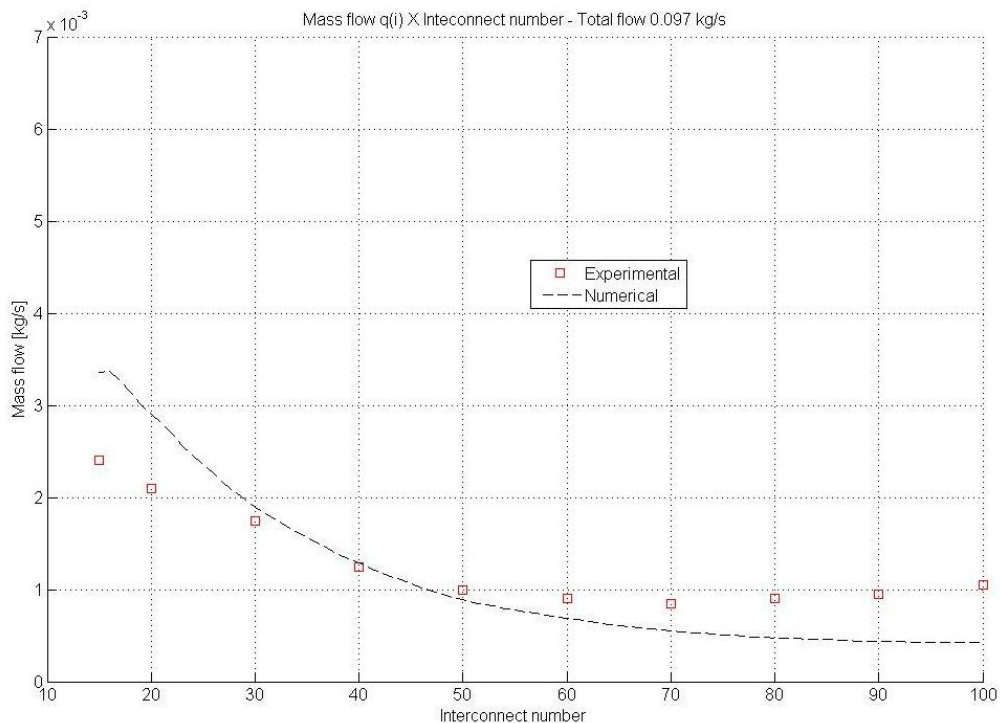


Figure 7: Comparison between model results and experimental data of Costamagna *et al.* (1994).

The numerical solution has good concordance with experimental data mainly for the interconnects between 30 to 70. Nevertheless, the numerical solution is not able to accompany the inlet effects as showed for interconnects between 15 to 30 and also for those between from 70 to 100.

#### 3.2. Tridimensional model results

The combination of a high aspect ratio with a relatively big domain led to a time-consuming processing, with more than 72 hours, using three dual core computers and 12 GB memory.

Basing on 0,25 mm mesh results, the flow distribution is analyzed in each of the channels, for interconnects 1, 5 and 10. The Fig. 8 presents the flow distribution for channels of these interconnects. The channel 1 is the most distant from the plane symmetry, highlighted in Fig. 2, while the channel 4 is the nearest.

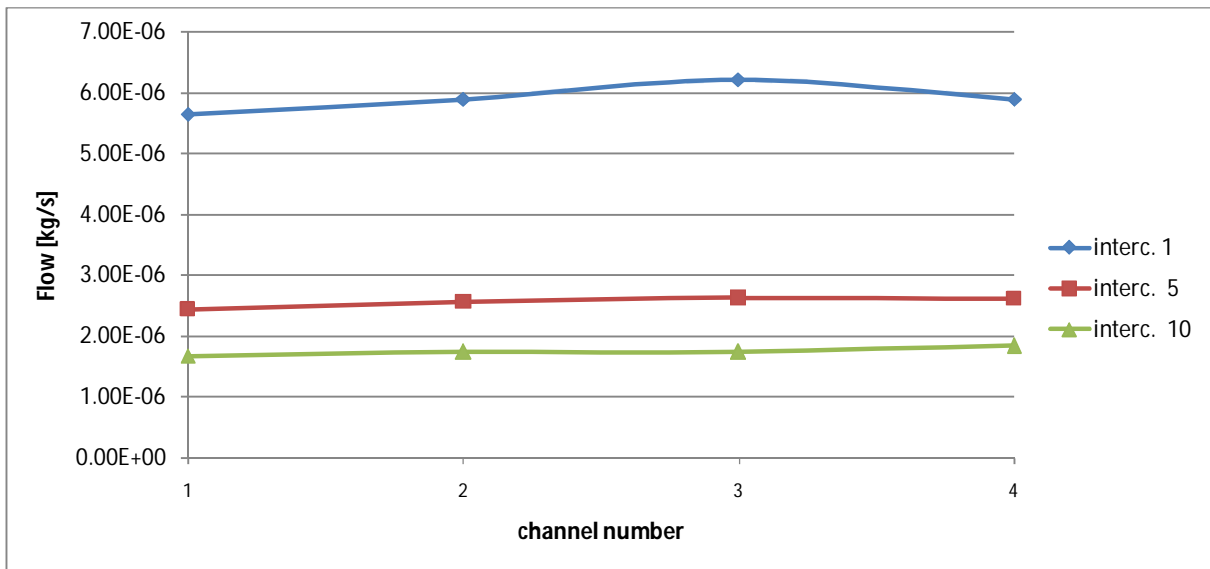


Figure 8: Comparison between flow distributions in each channel.

The Fig. 8 shows that, for a given interconnect, the flow remains almost constant in each of their channels, mostly for the interconnects 5 and 10. An analog behavior between the non analyzed interconnects is really expected.

The Fig. 9 shows the relative error of flows in the interconnects channels if compared to the homogenous distribution. The homogenous distribution is a hypothetical case, where the inlet flow is equally divided between all interconnects and channels.

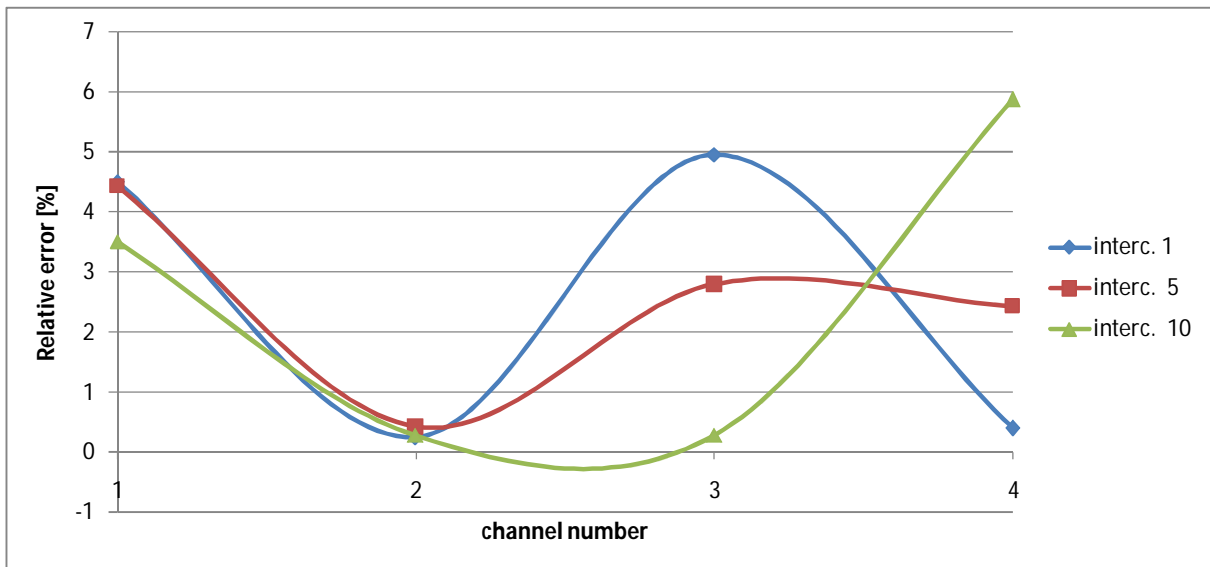


Figure 9: Relative error to homogenous distribution in channels.

The Fig. 9 shows that the stack has some heterogeneity grade, due to its geometry, as expected. It is possible to observe that the heterogeneity is relatively small, achieving values up to 6% largers if compared to homogeneous distribution.

The obtaining of a more homogenous flow distribution between interconnects could be possible, if a smaller diameter enlargement of manifolds was done. To a better investigation of the flow distribution along a given interconnect, it should be necessary to evaluate the influence of the diameter manifold and the relative position of this on the channels.



The pressures on inlet and outlet manifolds increase in an asymptotic way. For the inlet manifold, the pressure reaches up to 51 Pa, whereas the maximum value is equal to 45 kPa for the outlet manifold.

#### 4. CONCLUSION

This work evaluates flow distribution between the interconnects of a SOFC stack and along the channels of each of these interconnects. The analysis is conducted with a tridimensional model validated with experimental data available on specific literature. The validation of the model presents coherent results closed to experimental data.

The analysis indicates that the current design has a flow distribution with a relatively low heterogeneity between interconnects and also on their channels. Nevertheless, it could be possible to achieve distributions even more homogenous through changes of inlet manifolds diameters and of their relative position to channels of interconnects.

The model is a powerful tool to describe the stream in a stack. Later on, the heat transfer and the chemical reactions should be implemented on the model in order to have a better approach between the model and the experimental conditions.

#### 5. ACKNOWLEDGEMENTS

The authors thank CAPES and CEMIG for the financial support.

#### 6. REFERENCES

- Andrade, S. T. de P.; Bortolus, M. V.; Brant, M. C.; Domingues, R. Z.; Matencio, T., 2008, "Tridimensional modeling of solid oxide fuel cells", *Materia*, Vol. 13, N. 13, pp. 462-479.
- Autissier, N., Larrain, D., Van Herle, J., Farat, D., 2004, "CFD simulation tool for solid oxide fuel cells", *Journal of Power Source*, Vol. 131, pp. 313-319.
- Bove, R., Ubertini, S., 2006, "Modeling solid oxide fuel cell operation: Approaches, techniques and results", *Journal of Power Sources*, Vol. 159, pp. 543a-559a.
- Chyou, Y, Chung, T. , Chen, J, Shie, R., 2005, "Integrated thermal engineering analyses with heat transfer at periphery of planar solid oxide fuel cell", *Journal of Power Sources*, Vol. 139, pp. 126-140.
- Costamagna, P., Arato, E., Achenbach, E., Reus, U., 1994, "Fluid dynamic study of fuel cell devices: simulation and experimental validation", *Journal of Power Sources*, Vol. 52, pp. 243-249.
- Gubner, A., Nguyen-Xuan, T., Bram, M., Remmel, J., Haart, L.G.J., 2006, "Lightweight Cassette Type SOFC Stacks for Automotive Applications", 7th European SOFC Forum, Lucerne, Switzerland.
- Kakaç, S., Pramuanjaroenkij, A., Zhou, X., 2007, "A review of numerical modeling of solid oxide fuel cells". *International Journal of Hydrogen Energy*, Vol. 32, pp. 761-786.
- Malalasekera, W., Versteeg, H.K., 1995, "An introduction to computational fluid dynamics. The finite volume method", Prentice Hall, Harlow, 257 p.
- Patankar, S.V. ,1980, "Numerical heat transfer and fluid flow", Hemisphere Publishing Corporation, New York, USA, 197 p.
- Yakabe, H., Hishinuma, M., Uratani, M., Matsuzaki, Y., Yasuda, I., 2000, "Evaluation and modeling of performance of anode-supported solid oxide fuel cell", *Journal of Power Sources*, Vol. 86, pp. 423-431.
- Yokoo, M., Tabata, Y., Yoshida, Y., Hayashi, K., Nozaki, Y., Nozawa, K., Arai, H., "Highly efficient and durable anode-supported SOFC stack with internal manifold structure", *Journal of Power Sources*, Vol. 178, pp.59-63.
- Vandersteen, J.D.J., Kenney, B., Pharoah, J.G. and Karan, K., 2004, "Mathematical Modelling of the Transport Phenomena and the Chemical/ Electrochemical Reactions in Solid Oxide Fuel Cells: A Review." Canadian Hydrogen and Fuel Cells Conference.
- Van Herle, J., Larrain, D., Autissier, N., Wuillemin, Z., Molinelli, M., Favrat, D., 2005, "Modeling and experimental validation of solid oxide fuel cell materials and stacks", *Journal of the European Ceramic Society*, Vol. 25, pp. 2627-2632.
- Zitney, S.E., Prinkey, M.T., Shahnam, M. et al, 2004, "Coupled CFD and process simulation of a fuel cell auxiliary power unit", *Proceedings of Fuel Cell Science, Engineering and Technology*, pp. 339-345.